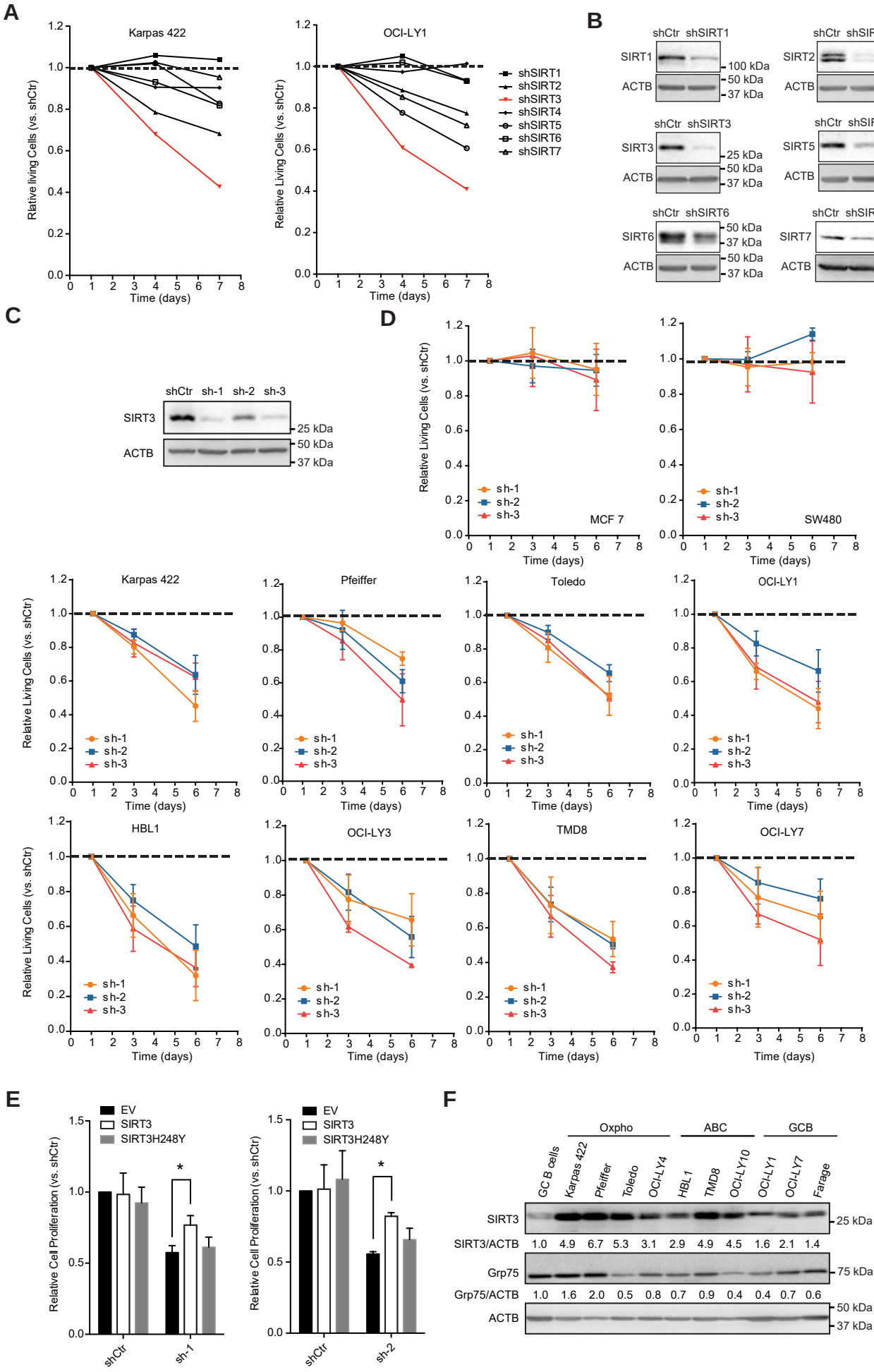
A
Karpas 422
OCI-LY1
Rlative living Cells (vs. shCtr)
Relative Living Cells (vs. shCtr)
Time (days)
shSIRT1
shSIRT2
shSIRT3
shSIRT4
shSIRT5
shSIRT6
shSIRT7
B
shCtr shSIRT1
shCtr shSIRT2
shCtr shSIRT3
shCtr shSIRT5
shCtr shSIRT6
shCtr shSIRT7
SIRT1
SIRT2
SIRT3
SIRT5
SIRT6
SIRT7
ACTB
100 kDa
50 kDa
37 kDa
25 kDa
C
shCtr sh-1 sh-2 sh-3
SIRT3
ACTB
D
Relative Living Cells (vs. shCtr)
MCF 7
SW480
Time (days)
sh-1
sh-2
sh-3
Karpas 422
Pfeiffer
Toledo
OCI-LY1
HBL1
OCI-LY3
TMD8
OCI-LY7
E
EV
SIRT3
SIRT3H248Y
Relative Cell Proliferation (vs. shCtr)
shCtr
sh-1
sh-2
F
Oxpho
ABC
GCB
GC B cells
Karpas 422
Pfeiffer
Toledo
OCI-LY4
HBL1
TMD8
OCI-LY10
OCI-LY1
OCI-LY7
Farage
SIRT3
SIRT3/ACTB
1.0 4.9 6.7 5.3 3.1 2.9 4.9 4.5 1.6 2.1 1.4
Grp75
Grp75/ACTB
1.0 1.6 2.0 0.5 0.8 0.7 0.9 0.4 0.4 0.7 0.6
ACTB
25 kDa
75 kDa
50 kDa
37 kDa

Figure S1 related to Figure 1.

(A) Karpas 422 and OCI-LY1were transduced with shRNA against the seven members of the sirtuin family of proteins. Cell proliferation was estimated by calculating the relative proportion of YFP+ cells among live cells ($DAPI^-$). YFP percentages were normalized to the first time point.

(B) Western blots were performed in the same cells in **Figure S1A** using the respective antibodies to each sirtuin to validate knockdown. SIRT4 is not shown since it was not detectable in these cells at baseline.

(C) Western blot analysis to validate efficiency of SIRT3 knockdown by three different SIRT3 shRNAs in Karpas 422 cells. ACTB was used as a loading control.

(D) Plots corresponding to data summarized in Figure 1A. The indicated cell lines were transduced with three different SIRT3 shRNA. Flow cytometry was used to determine the relative proportion of YFP^+ viable cells ($DAPI^-$) at different time points. Data were normalized to cells transduced with control shRNA (dashed line).

(E) Karpas 422 cells were transduced with lentiviruses expressing control (EV, empty vector), SIRT3 or $SIRT3^{H248Y}$ mutant along with different shRNAs. Cell numbers were counted at day 8-10 after infection. Relative cell proliferations were calculated according to cell numbers normalized against control cells (shCtr-EV). SIRT3 or $SIRT3^{H248Y}$ contains sense mutations in shRNA targeted sequences.

(F) Western blots performed using SIRT3 antibodies in a panel of cell lines corresponding to different DLBCL subtypes. Purified human tonsillar germinal center (GC) B-cells were used as the normal control. GRP75 and ACTB antibodies were used as loading controls for mitochondrial and total protein respectively. Densitometry was performed by comparing the levels of SIRT3 and GRP75 in DLBCL cells to normal GC B cells.

*p value<0.05, **p value<0.01, ***p value <0.001. Error bars represent the mean +/- SD of three replicates.

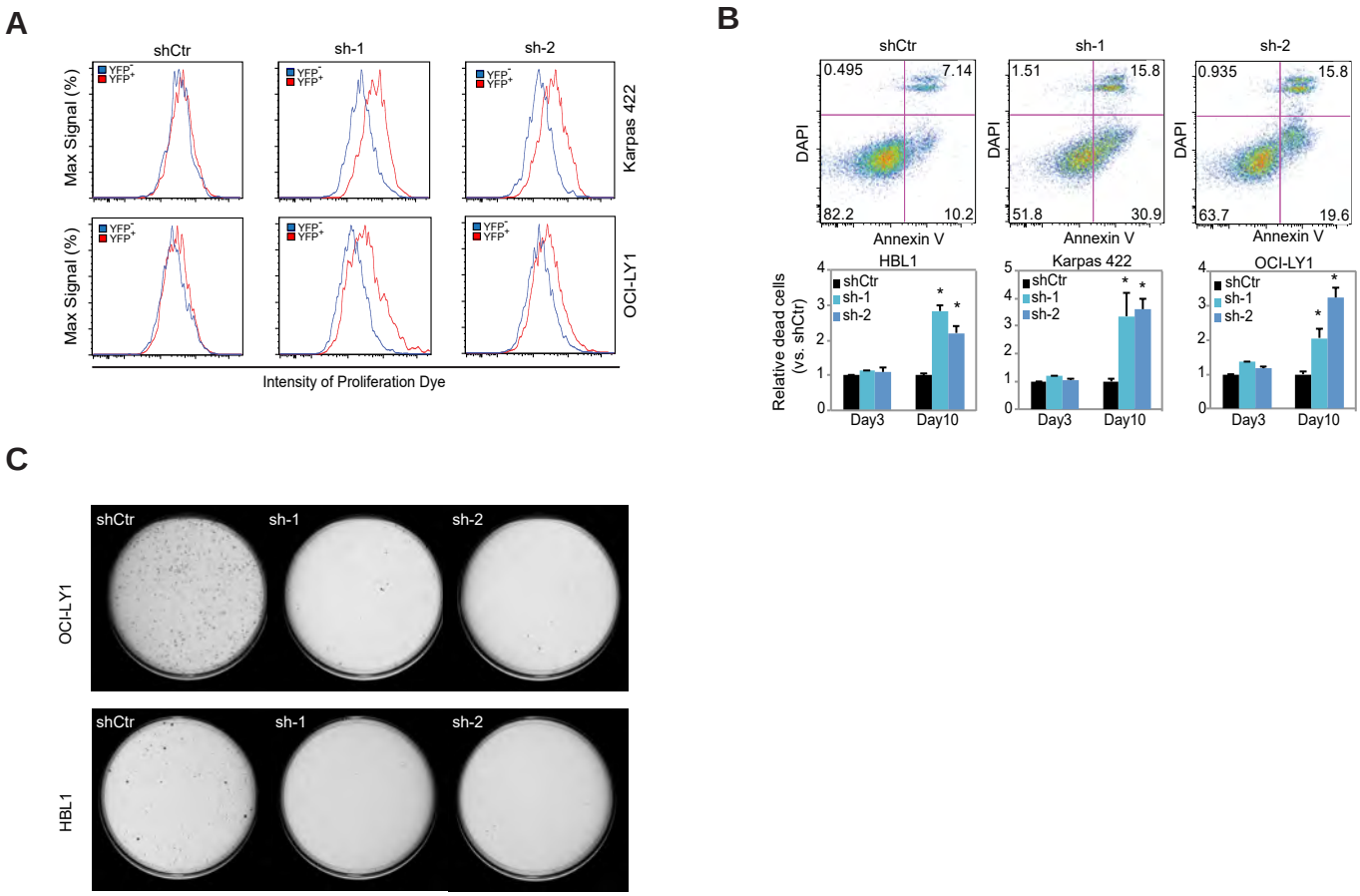

Figure S2 related to Figure 2.

(A) Karpas 422 and OCI-LY1 DLBCL cells were transduced with SIRT3 or control shRNA and stained with eflour 670 to assess frequencies of cell divisions. Flow cytometry analysis was performed five days later and the histograms represent staining for YFP^+ (red, transduced) and YFP^- (blue, non-transduced) cells cultured in the same flask shown respectively.

(B) Top, HBL1 cells were transduced with SIRT3 or control shRNAs as indicated. The fraction of cells undergoing apoptosis and cell death were estimated at 10 days later by flow cytometry analysis for DAPI and Annexin V. Bottom, a summarized representation of cell death using DAPI and Annexin flow cytometry in SIRT3 or control shRNA transduced HBL1, Karpas 422 and OCI-LY1 cells at two different time points (day 3 and 10 after virus transduction）.

(C) Photomicrographs comparing colony formation in OCI-LY1 and HBL1 cells transduced with SIRT3 or control shRNAs, 14 days after plating.

*p value<0.05. Error bars represent the mean +/- SD of three replicates.

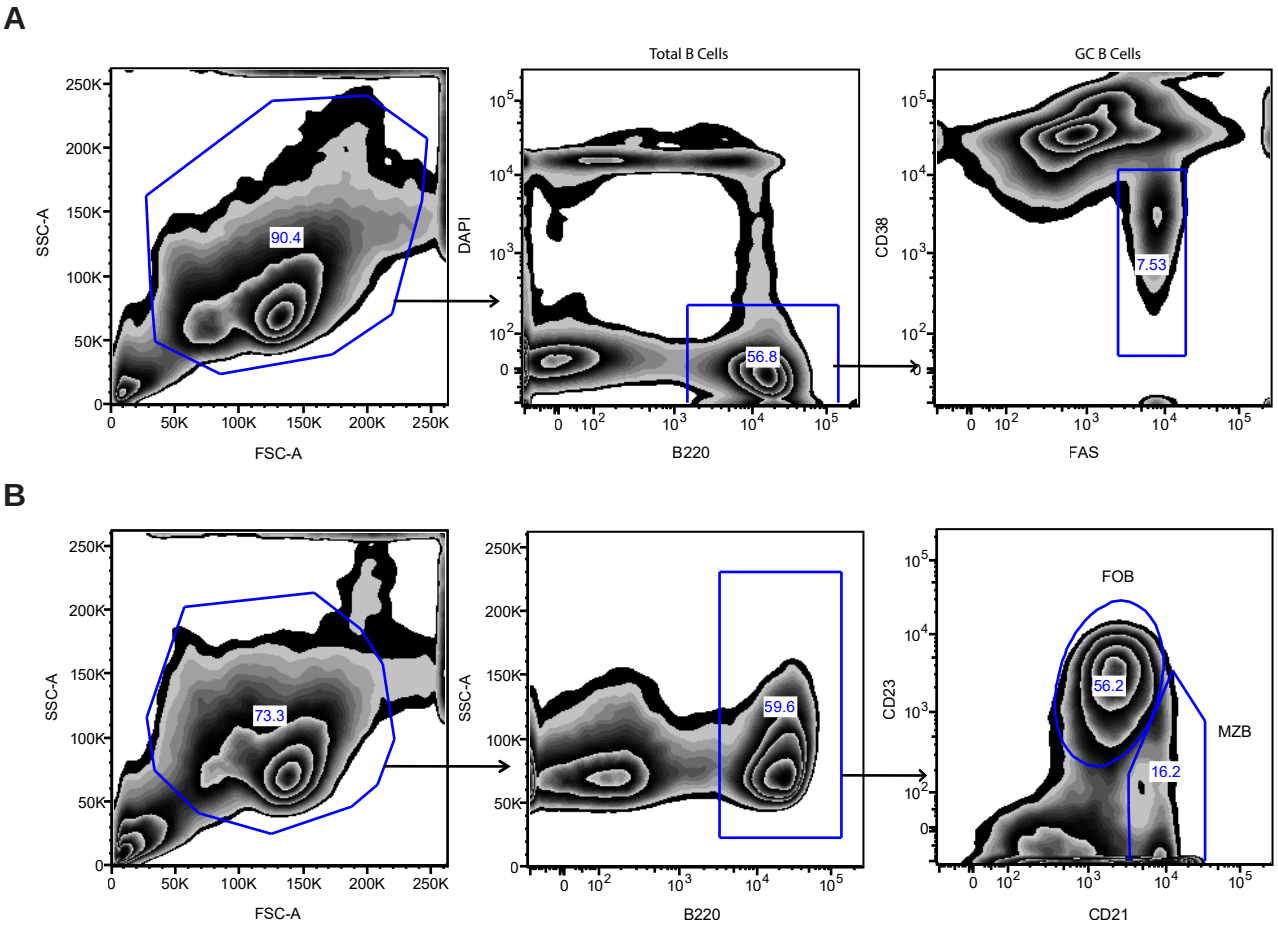

Figure S3 related to Figure 3.

(A) Flow cytometry gating strategies for total and GC B-cells among splenocytes.

(B) Flow cytometry gating strategies for follicular (FO) and marginal zone (MZ) B- cells among splenocytes.

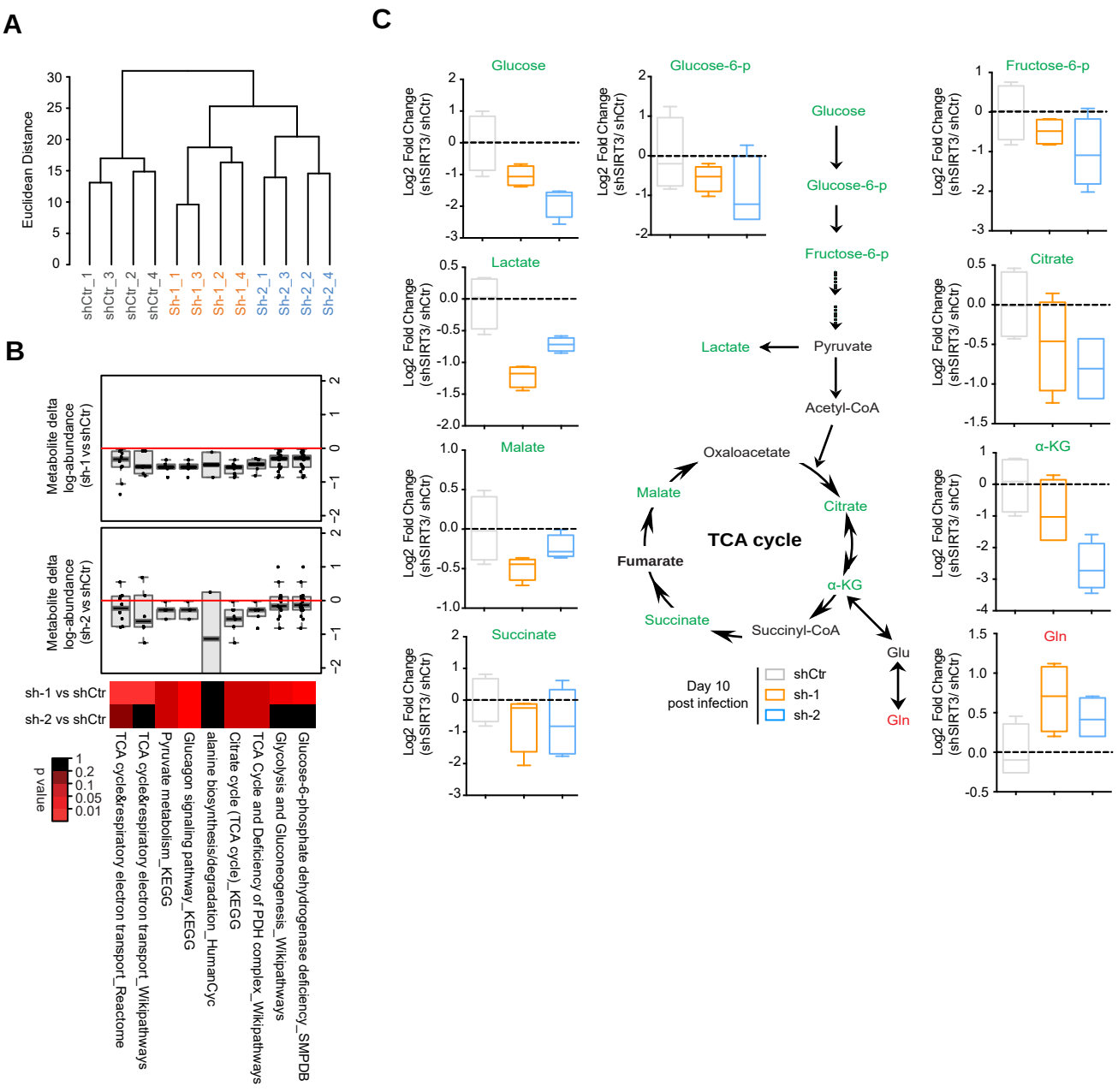

Figure S4 related to Figure 4.

(A) Metabolic profiling was performed in OCI-LY1 cells transduced with SIRT3 or control shRNA. The dendrogram shows the unsupervised hierarchical clustering of these metabolic profiles.

(B) Top, box plots show the relative abundance of the indicated sets of metabolites in SIRT3 vs control knockdown OCI-LY1 cells. Below, the heat map at the bottom shows the statistical significance of these differences by Wilcoxon test. Box plot represents lower quartile; median and upper quartile and whiskers show observed minimum and maximum values.

(C) Metabolic profiles of central carbon metabolites from SIRT3 depleted and control OCI-LY1 cells. Z scores were used to represent the relative abundance of the indicated metabolic intermediates. The increase and decrease in the levels of different metabolites is shown by red and green text, respectively. Box plot represents lower quartile; median and upper quartile and whiskers show observed minimum and maximum values.

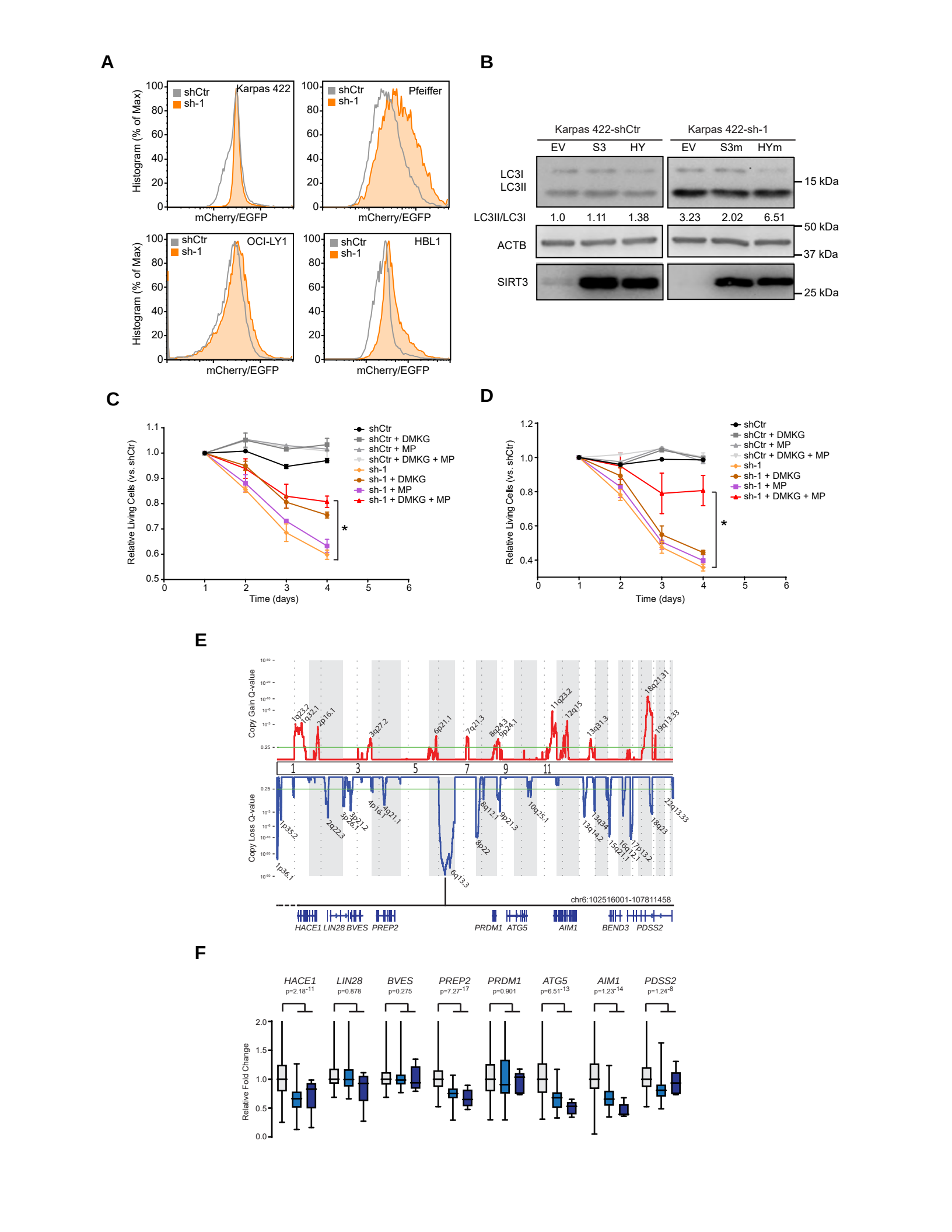
A
Karpas 422
Pfeiffer
OCI-LY1
HBL1
shCtr
sh-1
Histogram (% of Max)
mCherry/EGFP
B
Karpas 422-shCtr
Karpas 422-sh-1
EV
S3
HY
S3m
HYm
LC3I
LC3II
15 kDa
LC3II/LC3I
1.0
1.11
1.38
3.23
2.02
6.51
ACTB
50 kDa
37 kDa
SIRT3
25 kDa
C
Relative Living Cells (vs. shCtr)
Time (days)
shCtr
shCtr + DMKG
shCtr + MP
shCtr + DMKG + MP
sh-1
sh-1 + DMKG
sh-1 + MP
sh-1 + DMKG + MP
*
D
Relative Living Cells (vs. shCtr)
Time (days)
E
Copy Gain Q-value
Copy Loss Q-value
1q23.2
1q32.1
2p16.1
3q27.2
6p21.1
7q21.3
8q24.3
9p24.1
11q23.2
12q15
13q31.3
18q21.31
19q13.33
1p35.2
1p36.1
2q22.3
3p26.1
3p21.2
4p16.1
4q21.1
6q13.3
8q12.1
8p22
9p21.3
10q25.1
13q34
15q14.2
15q21.1
16q12.1
17p13.2
18q23
22q13.33
chr6:102516001-107811458
HACE1
LIN28
BVES
PREP2
PRDM1
ATG5
AIM1
BEND3
PDSS2
F
HACE1 p=2.18-11
LIN28 p=0.878
BVES p=0.275
PREP2 p=7.27-17
PRDM1 p=0.901
ATG5 p=6.51-13
AIM1 p=1.23-14
PDSS2 p=1.24-8
Relative Fold Change

Figure S5 related to Figure 5.

(A) Histograms showing mCherry/EGFP flow cytometry signals inSIRT3 (orange) and control shRNA transduced (grey) DLBCL cell lines.

(B) Western blots showed the autophagy levels (ratio of LC3II/LC3I) of Karpas 422 cells transduced with lentiviral vectors co-expressing control or SIRT3 shRNAs along with SIRT3 (S3), $SIRT3^{H248Y}$ (HY) or control(EV, empty vector). S3m and HYm indicate SIRT3 and $SIRT3^{H248Y}$, respectively, with sense mutations on shRNA targeted sequences. Densitometry results of LC3II/LC3I normalized to control cells (shCtr-EV).

(C) OCI-LY1 cells were transduced with SIRT3 or control shRNA and then cultured in media containing DMKG, MP or both for 4 days. The impacts of these treatments were assessed by determining the relative proliferation of transduced (YFP^+) vs non-transduced (YFP^-) cells and normalized to the first time point.

(D) HBL1 cells were transduced with SIRT3 or control shRNA and then cultured in media containing DMKG, MP or both for 4 days. Relative cell proliferation was assessed as in panel C.

(E) GISTIC2 analysis was performed for high-resolution single nucleotide polymorphism microarrays from 694 DLBCL tumors to identify significant DNA copy number gains (red) and losses (blue). The most significant DNA copy number alteration was identified at 6q21 ($Q=2.93x10^{-43}$). The peak of this alteration, corresponding to the smallest locus with the highest statistical significance, is highlighted (bottom) and contains 13 genes including *ATG5*.

(F) Matched gene expression profiling data were available for 249 cases for integrative analysis. Data were available for 8 genes, allowing us to interrogate the relationship between DNA copy number and transcript abundance. The expression of *ATG5* showed a dose-dependent decrease in expression with monoallelic (light blue) or biallelic (dark blue) deletion, resulting in a significantly lower level of transcript abundance compared to diploid tumors (grey). Box plot represents lower quartile; median and upper quartile and whiskers show observed minimum and maximum values.

Error bars represent the mean +/- SD of three replicates.

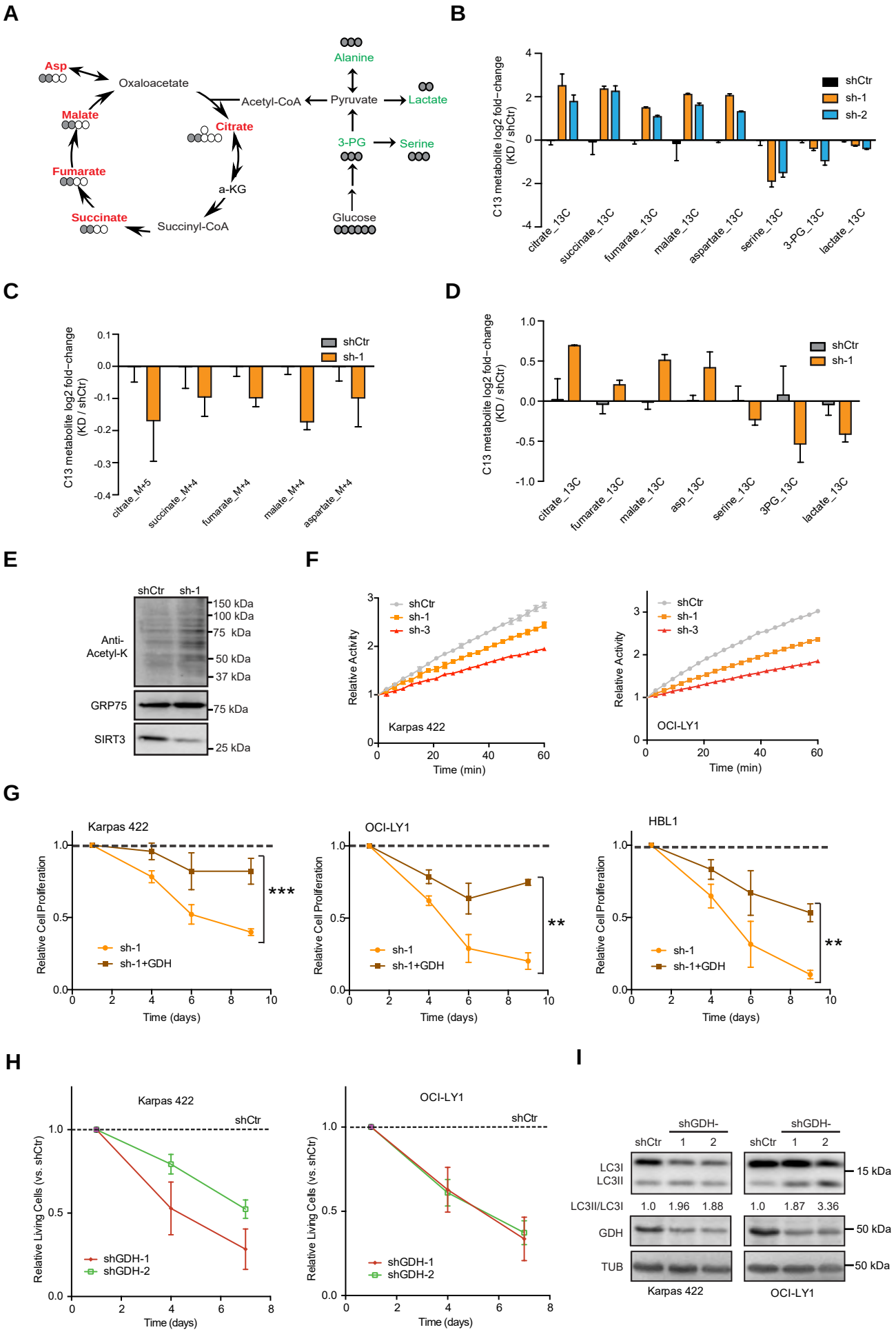
A
Asp
Oxaloacetate
Malate
Citrate
Acetyl-CoA
Alanine
Pyruvate
Lactate
3-PG
Serine
Fumarate
a-KG
Succinate
Succinyl-CoA
Glucose
B
C13 metabolite log2 fold−change (KD / shCtr)
shCtr
sh-1
sh-2
citrate_13C
succinate_13C
fumarate_13C
malate_13C
aspartate_13C
serine_13C
3-PG_13C
lactate_13C
C
C13 metabolite log2 fold−change (KD / shCtr)
shCtr
sh-1
citrate_M+5
succinate_M+4
fumarate_M+4
malate_M+4
aspartate_M+4
D
C13 metabolite log2 fold−change (KD / shCtr)
shCtr
sh-1
citrate_13C
fumarate_13C
malate_13C
asp_13C
serine_13C
3PG_13C
lactate_13C
E
shCtr
sh-1
Anti-Acetyl-K
GRP75
SIRT3
150 kDa
100 kDa
75 kDa
50 kDa
37 kDa
75 kDa
25 kDa
F
shCtr
sh-1
sh-3
Relative Activity
Karpas 422
Time (min)
shCtr
sh-1
sh-3
Relative Activity
OCI-LY1
Time (min)
G
Karpas 422
Relative Cell Proliferation
sh-1
sh-1+GDH
***
Time (days)
OCI-LY1
Relative Cell Proliferation
sh-1
sh-1+GDH
**
Time (days)
HBL1
Relative Cell Proliferation
sh-1
sh-1+GDH
**
Time (days)
H
Karpas 422
shCtr
Relative Living Cells (vs. shCtr)
shGDH-1
shGDH-2
Time (days)
OCI-LY1
shCtr
Relative Living Cells (vs. shCtr)
shGDH-1
shGDH-2
Time (days)
I
shCtr
shGDH-
1
2
shCtr
shGDH-
1
2
LC3I
LC3II
15 kDa
LC3II/LC3I
1.0
1.96
1.88
1.0
1.87
3.36
GDH
50 kDa
TUB
50 kDa
Karpas 422
OCI-LY1

Figure S6 related to Figure 6.

(A) Karpas 422 cells were transduced with SIRT3 or control shRNA followed by exposure to[U-^{13}C6] glucose. The increase or decrease of glycolytic and TCA cycle intermediate products are indicated by red and green text respectively. Carbon atom (^{13}C in grey and ^{12}C in white circles) transitions and tracers were used to detect glucose flux through the TCA cycle.

(B) Relative incorporation of ^{13}C glucose in TCA cycle metabolites in Karpas 422 cells transduced with SIRT3 vs. control shRNAs. The Y axis indicates log fold changes for incorporation of ^{13}C-metabolites.

(C) Relative incorporation of ^{13}C glutamine in TCA cycle metabolites in SIRT3 or control shRNA transduced OCI-LY1 cells. The Y axis indicates log fold changes for incorporation of ^{13}C-metabolites.

(D) Relative incorporation of ^{13}C glucose in the TCA cycle metabolites in SIRT3 or control shRNA transduced OCI-LY1 cells. The Y axis indicates log fold changes for incorporation of ^{13}C-metabolites.

(E) Karpas 422 cells were transduced with SIRT3 or control shRNA, followed by isolation of mitochondria and western blot using acetyl-lysine antibodies. GRP75 Western blots were performed as a loading control for mitochondrial protein.

(F) Graphs showing GDH activity following SIRT3 knockdown in Karpas 422 and OCI-LY1 cells compared to control shRNA.

(G) Graphs showed the cell proliferations of DLBCL cells with lentiviruses expressing SIRT3 shRNA (sh-1), both SIRT3 shRNA and GDH(sh-1+GDH) and control shRNA (the dash line). Relative cell proliferation was measured by counting the cell numbers in each condition and time points, then data were normalized to cells transduced with control shRNA (dashed line).

(H) Karpas 422 (left) and OCI-LY1 (right) cells were transduced with GDH or control shRNA. Relative cell proliferation was measured by determining the relative proportion of GFP^{+} (GDH shRNAs) normalized to cells transduced with control shRNA (dashed line).

(I) Karpas 422 (left) and OCI-LY1 (right) cells were transduced with GDH or control shRNA. Western blots were performed using LC3, GDH and tubulin antibodies. Autophagy activation was determined by measuring the LC3II/LC3I ratios according to densitometry values. GDH knockdown was verified by GDH antibody Western blot. Tubulin (TUB) Western blot was performed as a loading control.

*p value<0.05, **p value<0.01, ***p value <0.001. Error bars represent the mean +/- SD of three replicates.

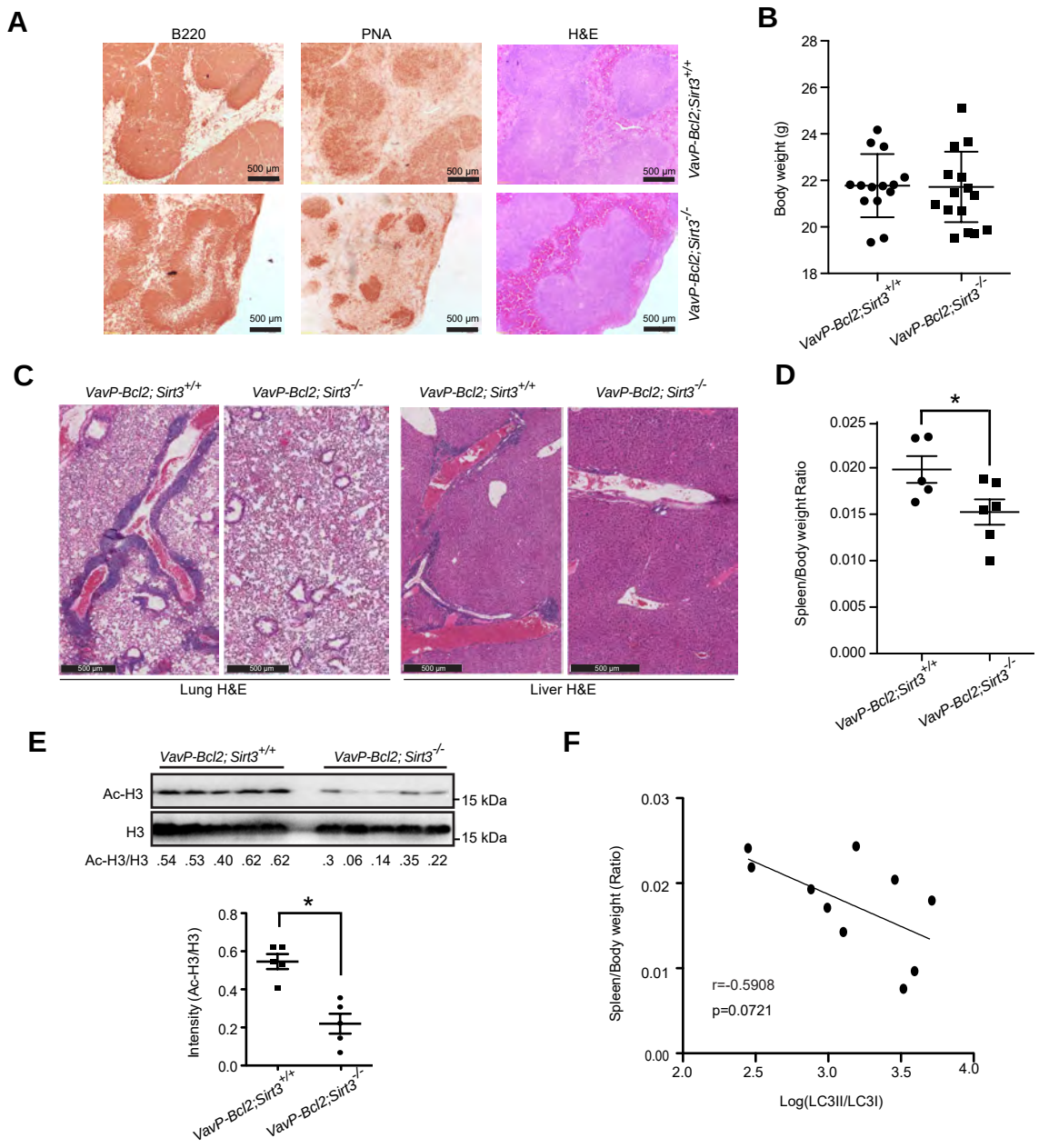

Figure S7 related to Figure 7.

(A) Immunohistochemical staining of spleen sections derived from 5-6 month old *VavP-Bcl2;Sirt3*$^{+/+}$ and *VavP-Bcl2;Sirt3*$^{-/-}$ mice with B220, PNA and H&E. Scale: 1 mm.

(B) Comparison of body weights in the two groups of recipient mice with *VavP-Bcl2;Sirt3*$^{+/+}$ and *VavP-Bcl2;Sirt3*$^{-/-}$ bone marrow cells. Data were collected from recipient mice of 110 days post bone marrow transplantation.

(C) Hematoxylin and Eosin (H&E) staining of lung and liver sections derived from recipient mice with *VavP-Bcl2;Sirt3*$^{+/+}$ and *VavP-Bcl2;Sirt3*$^{-/-}$ bone marrow cells. Scale: 500 μM.

(D) Comparison of spleen/body weight from recipient mice with *VavP-Bcl2;Sirt3*$^{+/+}$ and *VavP-Bcl2;Sirt3*$^{-/-}$ bone marrow cells at 150 days post bone marrow transplantation.

(E) Top, western blot analysis performed with acetyl-H3(Ac-H3) and pan H3 antibodies in *VavP-Bcl2;Sirt3*$^{-/-}$ vs. *VavP-Bcl2;Sirt3*$^{+/+}$ splenocytes. Densitometry values are shown for Ac-H3 normalized to total H3 abundance. Bottom, quantitative summary of Ac-H3/H3 ratios from *VavP-Bcl2;Sirt3*$^{+/+}$ and *VavP-Bcl2;Sirt3*$^{-/-}$ splenocytes. Densitometry results were calculated from the Western blot (top).

(F) Correlations of spleen/body weight ratios and LC3II/LC3I ratios in splenocytes derived from *VavP-Bcl2;Sirt3*$^{+/+}$ and *VavP-Bcl2;Sirt3*$^{-/-}$ mice.

*p value<0.05. Error bars represent the mean +/- SD of three or more replicates.

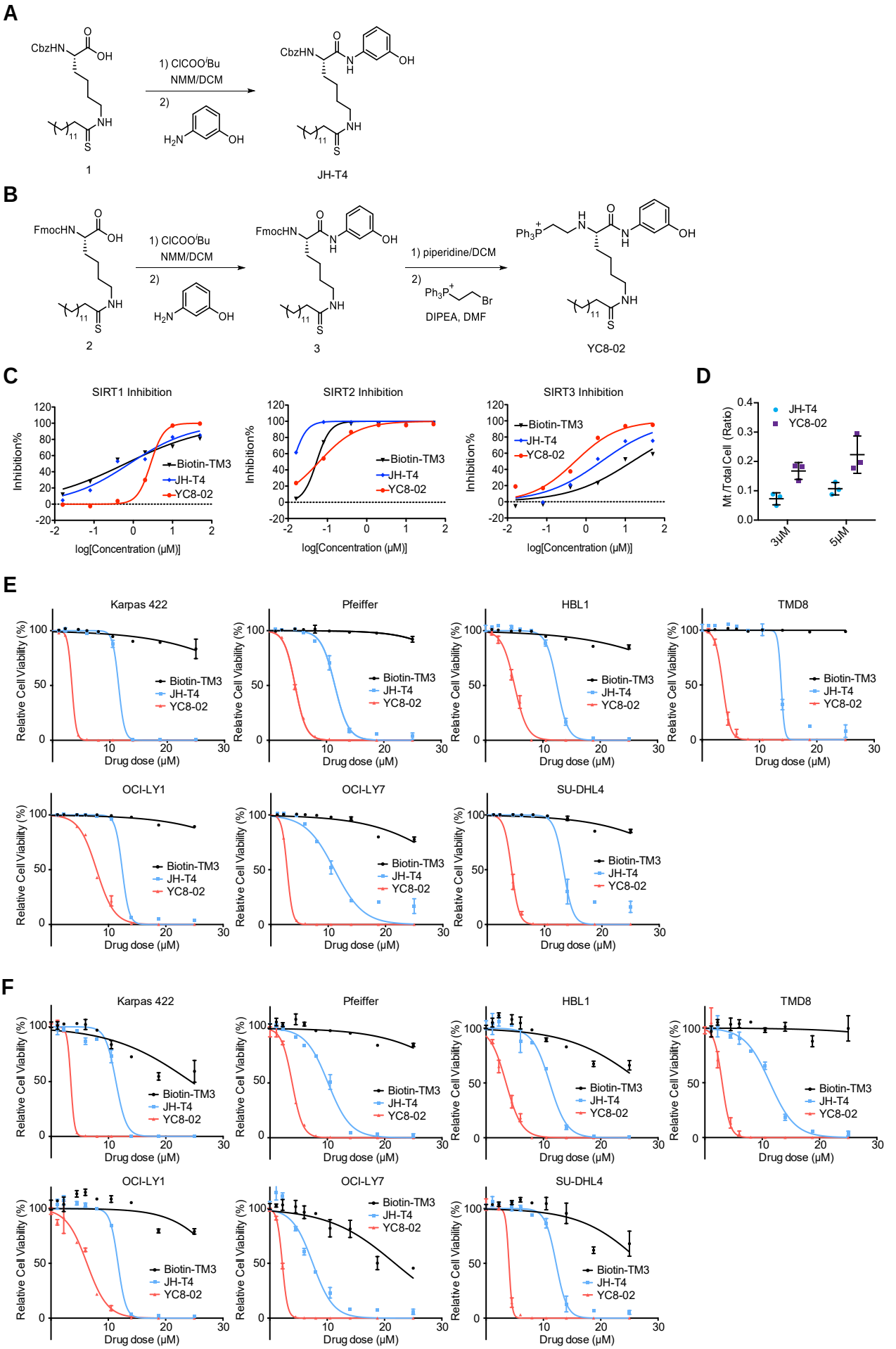
A
CbzHN
OH
NH
S
1) ClCOO^{t}Bu
NMM/DCM
2)
H_2N
OH
1
JH-T4
B
FmocHN
1) piperidine/DCM
2)
Ph_3P^+
Br
DIPEA, DMF
2
3
YC8-02
C
SIRT1 Inhibition
SIRT2 Inhibition
SIRT3 Inhibition
Inhibition%
log[Concentration (μM)]
Biotin-TM3
JH-T4
YC8-02
D
Mt /Total Cell (Ratio)
3μM
5μM
E
Karpas 422
Pfeiffer
HBL1
TMD8
OCI-LY1
OCI-LY7
SU-DHL4
Relative Cell Viability (%)
Drug dose (μM)
F

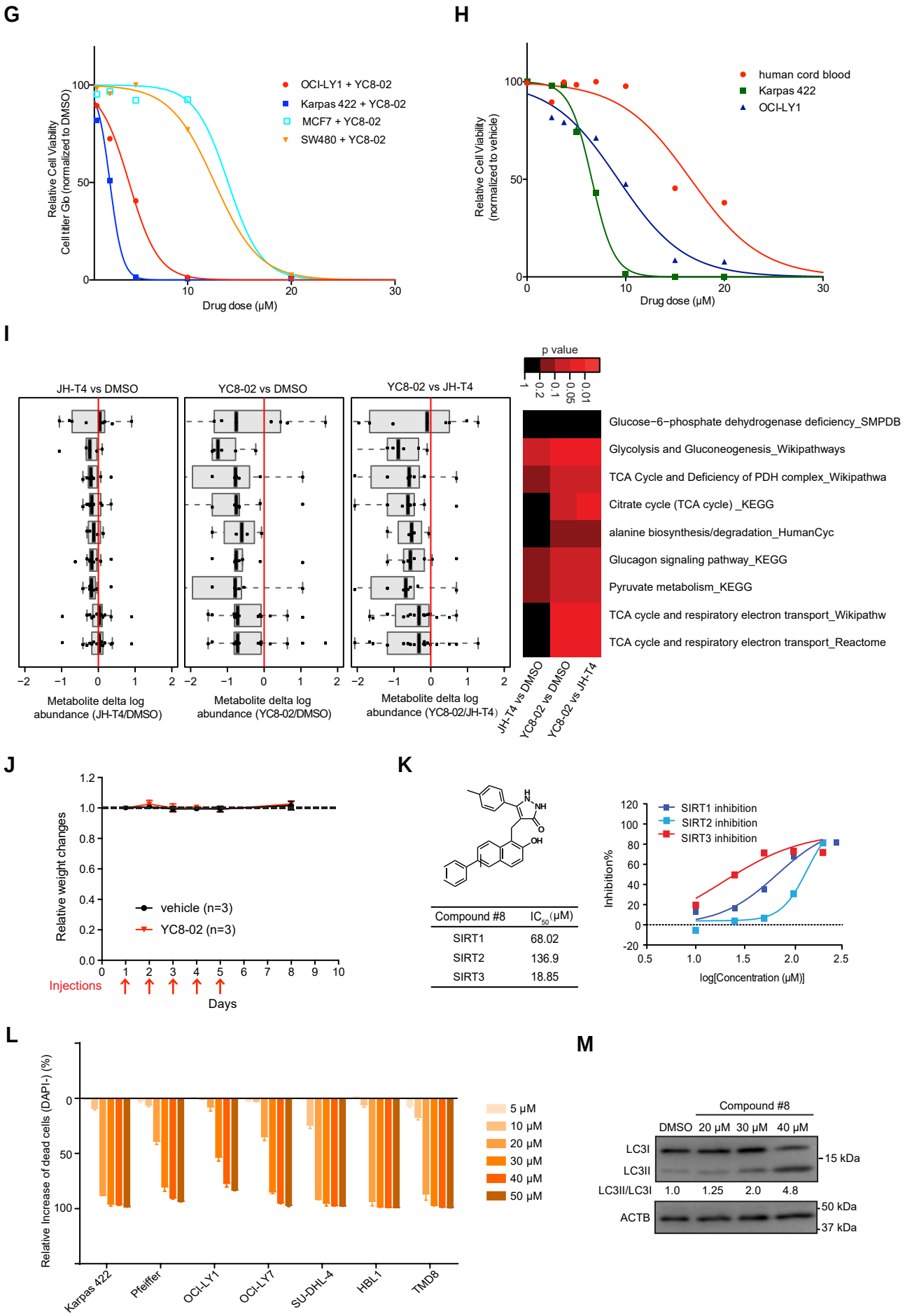
G
Relative Cell Viability
Cell titer Glo (normalized to DMSO)
OCI-LY1 + YC8-02
Karpas 422 + YC8-02
MCF7 + YC8-02
SW480 + YC8-02
Drug dose (μM)
H
Relative Cell Viability
(normalized to vehicle)
human cord blood
Karpas 422
OCI-LY1
Drug dose (μM)
I
JH-T4 vs DMSO
YC8-02 vs DMSO
YC8-02 vs JH-T4
p value
Metabolite delta log abundance (JH-T4/DMSO)
Metabolite delta log abundance (YC8-02/DMSO)
Metabolite delta log abundance (YC8-02/JH-T4)
Glucose−6−phosphate dehydrogenase deficiency_SMPDB
Glycolysis and Gluconeogenesis_Wikipathways
TCA Cycle and Deficiency of PDH complex_Wikipathwa
Citrate cycle (TCA cycle) _KEGG
alanine biosynthesis/degradation_HumanCyc
Glucagon signaling pathway_KEGG
Pyruvate metabolism_KEGG
TCA cycle and respiratory electron transport_Wikipathw
TCA cycle and respiratory electron transport_Reactome
J
Relative weight changes
vehicle (n=3)
YC8-02 (n=3)
Injections
Days
K
Compound #8
IC50(μM)
SIRT1 68.02
SIRT2 136.9
SIRT3 18.85
SIRT1 inhibition
SIRT2 inhibition
SIRT3 inhibition
Inhibition%
log[Concentration (μM)]
L
Relative Increase of dead cells (DAPI-) (%)
5 μM
10 μM
20 μM
30 μM
40 μM
50 μM
Karpas 422
Pfeiffer
OCI-LY1
OCI-LY7
SU-DHL-4
HBL1
TMD8
M
Compound #8
DMSO 20 μM 30 μM 40 μM
LC3I
LC3II
15 kDa
LC3II/LC3I 1.0 1.25 2.0 4.8
ACTB
50 kDa
37 kDa

Figure S8 related to Figure 8.

(A) Chemical synthesis of JH-T4.

(B) Chemical synthesis of YC8-02.

(C) *In vitro* deacetylase activity assays were performed to determine the inhibitory activity of Biotin-TM3, JH-T4 and YC8-02 on SIRT1, 2 and 3.

(D) Karpas 422 cells were treated with JH-T4 or YC8-02 at a concentration of 3 or 5 μM for 1hr. Total cell and mitochondrial fractions where assessed by HPLC.

(E) Dose response curves representing the percentage of viable cells ($DAPI^-$) among the indicated cells lines after treatment with Biotin-TM3, JH-T4 or YC8-02 for 48 hr.

(F) Dose response curves representing the cell numbers among the indicated cell lines after treatment with Biotin-TM3, JH-T4 or YC8-02 for 48 hr.

(G) The indicate cell lines were exposed to increasing concentrations of YC8-02 for 72 hours and viability determined by ATP luminescence assay. The Y axis reflects the proportion of viable cells in each case.

(H) Dose response curves representing the cell viability (CelltiterGlo™) after 24 hours YC8-02 treatment in DLBCL cell lines and human cord blood cells.

(I) Metabolic profiling was performed in Karpas 422 cells treated with YC8-02, JH-T4 or vehicle (DMSO). The boxplot shows the relative change in metabolite abundance of the indicated comparisons, whereas the heatmap shows the statistical significance of these changes (Wilcoxon test). Box plot represents lower quartile; median and upper quartile and whiskers show observed minimum and maximum values.

(J) Toxicity study where C57BL/6J mice were treated with YC8-02 or vehicle via IP injection once per day for 5 days (shown as red arrows below x axis). Animals were weighed every day before injection and relative change in weight is shown on the Y axis.

(K) Top left, structural formula of compound #8. Bottom left, Compound #8 IC_{50} values for SIRT1, SIRT2 and SIRT3. Right, dose response curves for *in vitro* inhibition of SIRT1, 2 and 3 deacetylase activity by compound #8.

(L) Relative proportion of dead cells among the indicated DLBCL cell lines treated with compound #8 for 48 hr. Cell viability was quantified by flow-cytometry using DAPI staining.

(M) Karpas 422 cells were treated with compound #8 for 40 hr and Western blots performed using LC3 and ACTB antibodies. Autophagy activation was evaluated by determining LC3II/LC3I ratios by densitometry, normalized to that in vehicle (DMSO) treated cells.

Error bars represent the mean +/- SD of three replicates.